

# Nested Game for Coupled Power System with Energy Sharing and Transportation System

Dongxiang Yan, Tongxin Li, Changhong Zhao, *Senior Member, IEEE*, Han Wang, Yue Chen, *Member, IEEE*

**Abstract**—The wide deployment of distributed renewable energy sources and electric vehicles can help mitigate climate change. This necessitates new business models in the power sector to hedge against uncertainties while imposing a strong coupling between the connected power and transportation networks. To address these challenges, this paper first proposes an energy sharing mechanism considering AC power network constraints to encourage local energy exchange in the power system. Under the proposed mechanism, all prosumers play a generalized Nash game. We prove that the energy sharing equilibrium exists and is socially optimal. Furthermore, a nested game is built to characterize the interactions both inside and between the power and transportation systems. Externally, the two systems are engaged in a Nash game because traffic flows serve as electric demands as a result of charging behaviors, and each driver pays the energy sharing price for charging. The nested game is then converted into a mixed-integer linear program (MILP) with the help of optimality conditions and linearization techniques. Numerical experiments validate the theoretical results and show the mutual impact between the two systems.

**Index Terms**—coupled power-transportation system, energy sharing, Wardrop user equilibrium, nested game

## NOMENCLATURE

### A. Acronyms

EV	Electric vehicle.
GV	Gasoline vehicle.
CS	Charging station.
OD	Origin-destination.
PV	Photovoltaic.
TS	Transportation system.
PS	Power system.
DER	Distributed energy resource.
MILP	Mixed-integer linear program.

### B. Indices and Sets

$\mathcal{E}_N$	Set of nodes in the power system.
$\mathcal{E}_L$	Set of lines in the power system.
$\mathcal{C}$	Set of CSs.
$C(i)$	Set of CSs powered by prosumer $i \in \mathcal{E}_N$ .

This work was supported by Shun Hing Institute of Advance Engineering (SHIAE) Fund No. 8115071. (*Corresponding Author: Yue Chen*)

D. Yan and Y. Chen are with the Department of Mechanical and Automation Engineering, the Chinese University of Hong Kong, Hong Kong SAR. (email: dongxiangyan@cuhk.edu.hk, yuechen@mae.cuhk.edu.hk)

T. Li is with the School of Data Science, The Chinese University of Hong Kong (Shenzhen), Shenzhen China. (email: litongxin@cuhk.edu.cn)

C. Zhao is with the Department of Information Engineering, the Chinese University of Hong Kong, Hong Kong SAR. (email: chzhao@ie.cuhk.edu.hk)

H. Wang is with the School of Electronic Information and Electrical Engineering, Shanghai Jiao Tong University, Shanghai 200240, China. (email: wanghan9894@sjtu.edu.cn)

$\mathcal{T}_N$	Set of nodes in the transportation system.
$\mathcal{T}_A$	Set of links in the transportation system.
$\mathcal{T}_R$	Set of origin nodes.
$\mathcal{T}_S$	Set of destination nodes.
$\mathcal{K}_g^{rs}$	Set of GV paths connecting OD pair $rs$ .
$\mathcal{K}_e^{rs}$	Set of EV paths connecting OD pair $rs$ .
$T_A^R$	Set of regular links.
$T_A^C$	Set of charging links.
$T_A^B$	Set of bypass links.
$S$	Set of partitions.

### C. Parameters

$p_i$	Renewable generator output at prosumer $i \in \mathcal{E}_N$ .
$d_i^f$	Fixed power demand at prosumer $i \in \mathcal{E}_N$ .
$\underline{D}_i/\bar{D}_i$	Lower/Upper bound of elastic demand at prosumer $i$ .
$m_a$	Market sensitivity.
$r_{ni}, x_{ni}$	Resistance and reactance of line $(n, i)$ .
$l_{ni}$	Squared current magnitude of line $(n, i)$ .
$v_n$	Squared voltage magnitude of node $n$ .
$\underline{P}_i/\bar{P}_i$	Lower/Upper bound of $P_i$ .
$\underline{Q}_i/\bar{Q}_i$	Lower/Upper bound of $Q_i$ .
$\underline{v}_i/\bar{v}_i$	Lower/Upper bound of $v_i$ .
$\bar{\ell}_{ni}$	Upper bound of $\ell_{ni}$ .
$q_g^{rs}/q_e^{rs}$	Total traffic flow between $r \in \mathcal{T}_R$ and $s \in \mathcal{T}_S$ for GV/EV.
$\delta_{akg}^{rs}/\delta_{ake}^{rs}$	Indicator variable for GV/EV.
$t_a^0$	Free travel time of link $a$ .
$h_a$	Free travel capacity of link $a$ .
$t_{a,c}^\mu$	Average service time at CS $c$ of link $a$ .
$t_{a,w}^c$	Maximum waiting time at CS $c$ of link $a$ .
$h_a^c$	Maximum allowable EV flow at CS $c$ of link $a$ .
$\gamma_a^c$	Electricity price of charging link $a$ with CS $c$ .
$E_b$	EV battery charging demand.
$\omega$	A constant converting time to monetary value.
$Z$	A integer parameter.
$c_m, A_1, A_2$	Constant coefficient matrices in compact form.
$D_{TS}, B_2$	Constant coefficient matrices in compact form.
$\lambda_{v,s}^{\min}/\lambda_{v,s}^{\max}$	Lower/Upper bounds of $\lambda_{v,s}$ for partition $s$ .
$D_{TS,s}^{\min}/D_{TS,s}^{\max}$	Lower/Upper bounds of $D_{TS,s}$ .
$ S $	Total partition number.

### D. Decision Variables

$d_i$	Elastic demand at node $i \in \mathcal{E}_N$ .
$D_i^T$	Total charging demand of links $a \in C(i)$ .
$q_i$	Sharing quantity of node $i \in \mathcal{E}_N$ .

$\lambda_i$	Sharing price for node $i \in \mathcal{E}_N$ .
$b_i$	Bid of prosumer $i \in \mathcal{E}_N$ in the sharing market.
$P_{ni}/Q_{ni}$	Active/Reactive power flow of line $(n, i)$ .
$U_i$	Utility of prosumer $i \in \mathcal{E}_N$ .
$f_{kg}^{rs}/f_{ke}^{rs}$	GV/EV traffic flow of a path $k \in \mathcal{K}_g^{rs}/\mathcal{K}_e^{rs}$ .
$x_a$	Aggregate traffic flow of link $a \in \mathcal{T}_A$ .
$x_{ag}/x_{ae}$	Aggregate GV/EV traffic flow of link $a \in \mathcal{T}_A$ .
$t_a$	Travel time on link $a \in \mathcal{T}_A$ .
$c_{kg}^{rs}/c_{ke}^{rs}$	Total cost of a path $k \in \mathcal{K}_g^{rs}/\mathcal{K}_e^{rs}$ for GV/EV.
$u_g^{rs}/u_e^{rs}$	Minimal cost from $r \in \mathcal{T}_R$ to $s \in \mathcal{T}_S$ for GV/EV.
$\xi^z, \eta^z$	Auxiliary variables.
$y_v$	Vector variable in compact form.
$\lambda_v, \mu_v$	Dual variables vectors in compact form.
$y_s$	Binary variable for partition $s \in S$ .
$\lambda_{v,s}$	Dual variable $\lambda_v$ for partition $s \in S$ .
$D_{TS,s}$	Variable $D_{TS}$ for partition $s \in S$ .
$\sigma$	Auxiliary variable to replace bilinear term.

## I. INTRODUCTION

**T**HE electrification of transportation systems together with massive deployment of clean sources such as renewable energy has been regarded as an important means of carbon emission reduction [1]. According to the Deloitte report, electric vehicle (EV) developed rapidly in the past decade and is expected to comprise 48%, 27%, and 42% of light-duty vehicle market shares in China, the U.S., and Europe, respectively, by 2030 [2]. Meanwhile, over 81,000 distributed wind turbines had been installed in the U.S. during 2003-2017 with a total capacity of 1,076 MW [3]. The residential solar photovoltaic (PV) panels also grew dramatically from 3,700 MW in 2004 to 150,000 MW in 2014 [4]. The impact of these trends is twofold: First, the proliferation of distributed energy resources (DERs) provides conventional consumers the ability to produce, turning them into proactive prosumers. The power system is changing from an operator-centric model to a prosumer-centric model. Secondly, the prosperity of EVs tightens the coupling of the power and transportation systems. Therefore, it is necessary to analyze the interaction between coupled power and transportation systems while considering the electric grid transformation.

For the former issue, instead of being dispatched centrally, prosumers prefer actively participate in energy management by efficiently configuring their production and consumption [5]. Many recent research turned to peer-to-peer energy sharing (trading) since it can unlock prosumers' flexibility to the maximum and provide enough incentive to get rid of the dependence on financial support [6]. Typical energy sharing mechanisms can be divided into optimization-based ones, cooperative game-based ones, and noncooperative game-based ones. Optimization-based mechanisms begin with a centralized problem and implement energy sharing with the help of distributed optimization algorithms, such as alternating direction method of multipliers [7]. To have a clearer economic interpretation, game theory is applied. Cooperative game-based mechanisms provide proper allocation rules so that all prosumers will spontaneously act towards the social optimum. Despite some well-known methods such as the Shapley value

[8], nucleolus [9], Nash bargaining [10], designing the allocation rule is challenging due to asymmetric information and privacy concerns. For non-cooperative game-based mechanisms, two typical models are Stackelberg games [11]–[13] and generalized Nash games [14]–[16]. Specifically, in the Stackelberg game [11], the operator moves first to decide on the electricity price and then prosumers choose their strategies. Reference [12] further considered prosumers' supply and demand ratios in the pricing decision of the operator [12]. A data-driven method was utilized to find a nearly optimal pricing strategy [13]. However, under the Stackelberg game setting, the flexibility of prosumers is limited to some extent since they are followers whose action sets are influenced by the operator (leader). In contrast, generalized Nash games allow prosumers to participate actively as leaders, which is the focus of this paper. A generalized demand function based mechanism was proposed with practical bidding algorithms [14]. Network constraints were further considered [15], [16]. However, they adopted simple DC power flow models, which are not accurate enough for the power distribution systems. Moreover, the above studies concentrated on analyzing the behaviors within power systems, whereas the interaction of multi-energy systems with energy sharing is implemented remains unexplored.

For the latter issue, a large number of EV charging stations (CSs) have been constructed in recent years to meet the growing EV charging needs. On the one hand, the routing of EV traffic flow for CSs will impact the road congestion of transportation systems [17]. On the other hand, the high charging demand from CSs can pose a threat to the distribution network operation [18]. Therefore, it is important to analyze the impact of EVs' traveling and charging behavior on the two systems' operation [19]. References [20] and [21] studied the optimal traffic-power flow using a mixed integer linear program (MILP). The EV scheduling strategies [22], the urban transportation network expansion planning [23], and the resilience enhancement [24] of coupled transportation and power systems were investigated. The above works assumed that both systems are under the control of the same operator. However, in reality, the two systems belong to different stakeholders and may have conflicting interests. A bi-level model was proposed to coordinate the two systems [25]. Reference [26] considered the decision-making of each system as an independent stakeholder. Iterative methods were proposed to search for the equilibrium, which, however, have no convergence guarantee. Besides, their power systems adopted a centralized operation model without taking into account the promising trend of energy sharing in the prosumer era.

This paper studies the interaction of coupled power and transportation systems with consideration of the strategic behavior within each system, i.e. the prosumers' strategic energy sharing behaviors in the power system and the EV drivers' strategic route selection behavior in the transportation system. The main contributions are twofold:

1) *Nested Game Model of Coupled Transportation and Power Systems.* We propose a nested game model to characterize the complex interactions of coupled power and transportation systems. In the power system, an effective energy sharing

mechanism is proposed under which all prosumers play a generalized Nash game. Different from the existing work, AC power network constraint is incorporated. In the transportation system, all drivers strategically select their routes to minimize their travel costs, which constitutes a Nash game. The charging load from EVs in the links with charging stations of the transportation system serves as the electric demand for one node in the power system, and the drivers pay the energy sharing prices derived from the energy sharing market clearing for charging. Hence, externally, there is a Nash game between the two systems.

2) *Method for Computing the Equilibrium.* To obtain the equilibrium of the proposed nested game, we first provide two equivalent optimization models to compute the equilibrium in the power and transportation systems, respectively, in Propositions 1 and 2. Then, to accelerate the computation, we linearize the nonlinear AC power network constraint via polyhedral approximation. Further, we replace the equivalent optimization model for energy sharing equilibrium in the power system with its *primal-dual optimality* condition. The resulting nonlinear terms are linearized by piecewise McCormick envelope and SOS2 variables. Finally, the equilibrium of the nested game can be solved by a MILP. Case studies show that the proposed method can greatly enhance the computational efficiency and avoid the disconvergence problem of the traditional methods.

## II. MATHEMATICAL FORMULATION

The structure of the coupled power and transportation systems is shown in Fig. 1. Each charging station (CS) in the transportation system is powered by a prosumer node in the power distribution system. When an EV goes to a CS, it receives a certain amount of energy. In the transportation system, we consider two kinds of vehicles: traditional gasoline vehicles (GV) and EVs. Each GV driver chooses the route that has the minimum travel time. Each EV driver chooses the route that can minimize its travel cost, which includes a cost proportional to the travel time and a cost related to the charging price. In the distribution power system, each prosumer node is equipped with a distributed renewable generator to supply its demand and to provide electricity for a CS in the transportation system. The prosumer nodes can share energy with each other so that the one with excess power can sell electricity to the one that lacks power. In general, the transportation system and the power system closely couple with each other. The traffic flow will influence the demand at the nodes of the power distribution system, which will further impact the energy sharing result. The energy sharing price affects the driving behavior of EV owners, which in turn influences the traffic flow in the transportation system. In the following, we will first introduce the game models inside the power and transportation systems, respectively; and then the nested game model considering the interactions of the two systems.

### A. Energy Sharing Equilibrium in Power System

The power system can be modeled as a connected graph  $\mathcal{G}_E = [\mathcal{E}_N, \mathcal{E}_L]$ , where  $\mathcal{E}_N$  and  $\mathcal{E}_L$  represent the set of nodes and power lines, respectively. Each prosumer node  $i$  has a

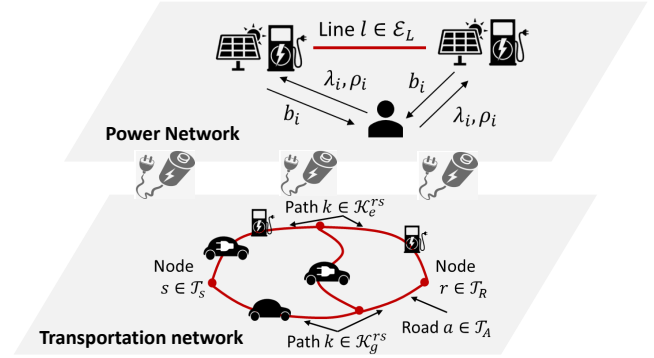


Fig. 1. Structure of the coupled power and transportation systems.

renewable generator whose output is  $p_i$ , fixed demand  $d_i^f$ , and elastic demand  $d_i \in [\underline{D}_i, \overline{D}_i]$ . Other nodes only have fixed demand. For notation conciseness, for the nodes with fixed demand, we let their  $p_i = 0$  and  $\underline{D}_i = \overline{D}_i = 0$ . Denote the set of CSs supplied by prosumer node  $i$  as  $C(i)$ , which imposes total power demand  $D_i^T$  by EVs. With the real-time renewable generator output  $p_i$ , the prosumer  $i \in \mathcal{E}_N$  can adjust its elastic demand  $d_i$  or share the amount of energy  $q_i$  with other prosumers at a price  $\lambda_i$  to maintain energy balancing. The utility of elastic demand can be represented by concave functions  $U_i(d_i), \forall i$ , so that  $-U_i(d_i), \forall i$  are convex functions. We propose an energy sharing mechanism as follows:

To participate in energy sharing, each prosumer  $i \in \mathcal{E}_N$  submits a bid  $b_i$  to the market operator, indicating its willingness to buy. The energy sharing market prices  $\lambda_i, \forall i \in \mathcal{E}_N$  and the sharing quantities  $q_i, \forall i \in \mathcal{E}_N$  will be determined according to the bids. Their relationship can be represented by a generalized demand function  $q_i = -m_a \lambda_i + b_i$ , where  $m_a > 0$  is the market sensitivity. It shows that given the same price  $\lambda_i$ , the prosumer will buy more if it has a higher willingness to buy (the higher  $b_i$ , the higher  $q_i$ ); the prosumer will buy less when energy is more expensive (the higher  $\lambda_i$ , the less  $q_i$ ). The market operator clears the market by solving:

$$\min_{\lambda_i, \forall i \in \mathcal{E}_N} \sum_{i \in \mathcal{E}_N} \lambda_i^2, \quad (1a)$$

$$\text{s.t. } (-m_a \lambda_i + b_i) \in \mathcal{F}_c, \quad (1b)$$

where

$$\mathcal{F}_c := \{q_i, \forall i \mid$$

$$P_{ni} - q_i - r_{ni} \ell_{ni} - \sum_{k:(i,k)} P_{ik} = 0, \forall (n, i) \in \mathcal{E}_L, \quad (2a)$$

$$Q_{ni} + Q_i - x_{ni} \ell_{ni} - \sum_{k:(i,k)} Q_{ik} = 0, \forall (n, i) \in \mathcal{E}_L, \quad (2b)$$

$$v_n - 2(r_{ni} P_{ni} + x_{ni} Q_{ni}) + (r_{ni}^2 + x_{ni}^2) \ell_{ni} = v_i, \forall (n, i) \in \mathcal{E}_L, \quad (2c)$$

$$P_{ni}^2 + Q_{ni}^2 \leq \ell_{ni} v_n, \forall (n, i) \in \mathcal{E}_L, \quad (2d)$$

$$\underline{P}_i \leq q_i \leq \overline{P}_i, \forall i \in \mathcal{E}_N, \quad (2e)$$

$$\underline{Q}_i \leq Q_i \leq \overline{Q}_i, \forall i \in \mathcal{E}_N, \quad (2f)$$

$$\underline{v}_i \leq v_i \leq \overline{v}_i, \forall i \in \mathcal{E}_N, \quad (2g)$$

$$0 \leq \ell_{ni} \leq \overline{\ell}_{ni}, \forall (n, i) \in \mathcal{E}_L \}. \quad (2h)$$

where  $Q_i$  is bus  $i$ 's reactive power injection,  $P_{ni}/Q_{ni}$  is the active/reactive power flow of line  $(n, i)$ ,  $r_{ni}/x_{ni}$  is the resistance/reactance, and  $\ell_{ni}/v_n$  is the squared current/voltage

magnitude. The objective function (1a) is designed to minimize the sum of square of the energy sharing prices. We will prove later in Proposition 1 that such a design can guarantee an equilibrium that is socially optimal. Constraints (2a)-(2d) describe the branch flow model. Second-order cone relaxation is applied, so the original equality constraint has been turned into the inequality constraint in (2d). Constraints (2e)-(2h) include the physical bounds of prosumer power injection capacities, squared bus voltages, and squared line current magnitude.

For each prosumer  $i \in \mathcal{E}_N$ , its net cost equals the energy sharing cost  $\lambda_i q_i$  (when  $q_i < 0$ , it means prosumer  $i \in \mathcal{E}_N$  will sell energy to the market and receive revenue  $-\lambda_i q_i$  minus its utility  $U_i(d_i)$ ). It can decide on the optimal values of  $d_i$  and  $b_i$  to minimize its net cost:

$$\min_{b_i, d_i} -U_i(d_i) + \lambda_i(-m_a \lambda_i + b_i), \quad (3a)$$

$$\text{s.t. } p_i - m_a \lambda_i + b_i = d_i + d_i^f + D_i^T, \quad (3b)$$

$$\underline{D}_i \leq d_i \leq \bar{D}_i. \quad (3c)$$

Constraint (3b) shows that the renewable generation plus the energy it buys from the energy sharing market can satisfy its fixed and elastic demands. Constraint (3c) is the demand adjustable range.

The aforementioned energy sharing mechanism can protect the privacy of both prosumers and the operator to some extent, since the network constraints (2a)-(2h) are known only to the operator and the individual capacity constraint (3c) is available only to the prosumer. If we take the market operator as a virtual player, then all prosumers and the operator play a generalized Nash game. A major feature that distinguishes the generalized Nash game from a standard Nash game is that both the objective function and the constraints of one player are influenced by the strategies of the other players [27]. Denote the objective function (1a) of the market operator as  $\Gamma_M(\lambda)$  and its feasible set as  $\mathcal{X}_M(b) := \{\lambda \mid (1b) \text{ is satisfied.}\}$ . Denote the objective function (3a) of each node as  $\Gamma_i(\lambda_i, b_i, d_i)$  and its feasible set as  $\mathcal{X}_i(\lambda_i) := \{(b_i, d_i) \mid (3b) - (3c) \text{ are satisfied.}\}$ .

**Definition 1.** (Energy Sharing Equilibrium) A profile  $(b^*, d^*, \lambda^*)$  is a *generalized Nash equilibrium* (GNE) of the energy sharing game (1) and (3) if and only if

$$\begin{aligned} \lambda^* &= \operatorname{argmin}_{\lambda \in \mathcal{X}_M(b^*)} \Gamma_M(\lambda) \\ (b^*, d^*) &= \operatorname{argmin}_{b_i, d_i \in \mathcal{X}_i(\lambda_i^*)} \Gamma_i(\lambda_i^*, b_i, d_i), \forall i \in \mathcal{E}_N \end{aligned} \quad (4)$$

In general, generalized Nash games are difficult to analyze, and there is no theoretical guarantee for the existence and uniqueness of an equilibrium. Moreover, as part of the power demand  $D_i^T$  comes from the transportation system, the interaction among the two systems constitutes another Nash game described later in Section II-C. This makes the problem even more sophisticated. In Section III, we will derive an equivalent optimization model in Proposition 1 for computing the generalized Nash equilibrium efficiently.

### B. Wardrop User Equilibrium in Transportation System

The transportation system can be modeled as a connected graph  $\mathcal{G}_T = [\mathcal{T}_N, \mathcal{T}_A]$ , where  $\mathcal{T}_N$  and  $\mathcal{T}_A$  represent the set of

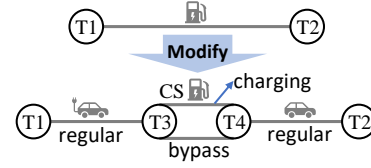


Fig. 2. Illustration of three types of links.

nodes and roads (links), respectively. Each road (link) is denoted by  $a \in \mathcal{T}_A$  and its traffic flow by  $x_a$ . Each driver needs to travel from an origin node  $r$  to a destination node  $s$ . Each origin-destination (OD) pair  $rs$  is connected by a set of paths. We consider two kinds of vehicles in the transportation system: GVs and EVs. The GV traffic flow of a path  $k \in \mathcal{K}_g^{rs}$  is  $f_{kg}^{rs}$  and the given total GV traffic flow from  $r$  to  $s$  is  $q_g^{rs} = \sum_{k \in \mathcal{K}_g^{rs}} f_{kg}^{rs}$ . Similarly, for EV traffic flow,  $q_e^{rs} = \sum_{k \in \mathcal{K}_e^{rs}} f_{ke}^{rs}$ . To characterize the relationship between  $f_{kg}^{rs}, f_{ke}^{rs}, \forall k, \forall (rs)$  and  $x_a$ , we introduce the indicator variable  $\delta_{akg}^{rs}$  ( $\delta_{ake}^{rs}$ ) for GVs (EVs).  $\delta_{akg}^{rs} = 1$  ( $\delta_{ake}^{rs} = 1$ ) if road  $a \in \mathcal{T}_A$  is part of the path  $k \in \mathcal{K}_g^{rs}$  ( $k \in \mathcal{K}_e^{rs}$ ); otherwise,  $\delta_{akg}^{rs} = 0$  ( $\delta_{ake}^{rs} = 0$ ). Therefore,

$$x_a = \underbrace{\sum_{rs} \sum_{k \in \mathcal{K}_g^{rs}} \delta_{akg}^{rs} f_{kg}^{rs}}_{x_{ag}} + \underbrace{\sum_{rs} \sum_{k \in \mathcal{K}_e^{rs}} \delta_{ake}^{rs} f_{ke}^{rs}}_{x_{ae}}, \quad \forall a \in \mathcal{T}_A \quad (5)$$

where  $\sum_{rs}$  is used to abbreviate  $\sum_r \sum_s$ . The travel time  $t_a$  on a link  $a \in \mathcal{T}_A$  depends on its aggregate traffic flow  $x_a$ .

There are two types of links: the regular link without a CS  $a \in \mathcal{T}_A^R$  and the charging link with a CS. When an EV travels on the charging link, it can choose to get charged at the CS or bypass the CS. To facilitate the modeling and analysis, the original network is modified by adding a bypass link in parallel to the charging link, as shown in Fig. 2. The charging link is denoted by  $a \in \mathcal{T}_A^C$  while the bypass link by  $a \in \mathcal{T}_A^B$ .  $\mathcal{T}_A = \mathcal{T}_A^R \cup \mathcal{T}_A^C \cup \mathcal{T}_A^B$ .

For the regular link  $a \in \mathcal{T}_A^R$ , we adopt the Bureau of Public Roads (BPR) function (6) to describe the travel time, which increases with the traffic flow [28].

$$t_a(x_a) = t_a^0 \left[ 1 + 0.15 \left( \frac{x_a}{h_a} \right)^4 \right] \quad (6)$$

where  $t_a^0$  and  $h_a$  are the free travel time and the capacity of link  $a$ . For a charging link ( $a \in \mathcal{T}_A^C$ ), the time spent on it is

$$t_a(x_a) = t_{a,\mu}^c + t_{a,w}^c \left( \frac{x_a}{h_a^c} \right)^3, \quad x_a \leq h_a^c \quad (7)$$

where  $t_{a,\mu}^c, t_{a,w}^c, h_a^c$  denote the average service time, the maximum waiting time at CS  $c \in \mathcal{C}$ , and the maximum allowable EV flow of CS  $c \in \mathcal{C}$  where  $\mathcal{C}$  is the set of CSs. The travel time on a bypass link  $a \in \mathcal{T}_A^B$  is assumed to be zero due to the very short length, i.e.,  $t_a(x_a) = 0, \forall a \in \mathcal{T}_A^B$ .

For a GV owner, its travel cost  $c_{kg}^{rs}$  on path  $k \in \mathcal{K}_g^{rs}$  between OD pair  $rs$  is only influenced by the travel time:

$$c_{kg}^{rs} = \sum_{a \in \mathcal{T}_A} \omega t_a(x_a) \delta_{akg}^{rs} \quad (8)$$

where  $\omega$  is the monetary cost of travel time.

For an EV owner, when deciding its route, it cares about two factors: the travel time and the charging price. Denote the charging price of the charging link  $a$  with CS  $c \in \mathcal{C}$  by  $\gamma_a^c$ , and

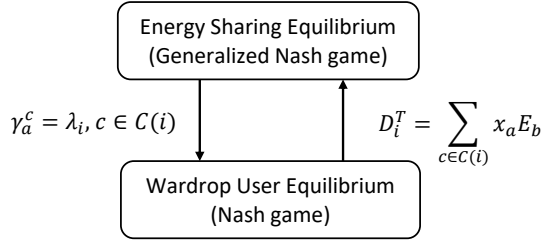


Fig. 3. Nested game of transportation and power systems.

we have  $\gamma_a^c = \lambda_i$  if CS  $c \in C(i)$ . The EV travel cost of a path  $k \in \mathcal{K}_e^{rs}$  is

$$c_{ke}^{rs} = \sum_{a \in \mathcal{T}_A} \omega t_a(x_a) \delta_{ake}^{rs} + \sum_{a \in \mathcal{T}_A^C} \gamma_a^c E_b \delta_{ake}^{rs} \quad (9)$$

where  $E_b$  represents an EV's charging demand, which is a constant, e.g., 20kWh.

Given the total traffic flow  $q_{rs}$  of all OD pairs  $rs$ , each driver will choose the route that can minimize its own travel cost. Meanwhile, the decisions of all drivers will affect the aggregate traffic flow  $x_a, \forall a \in \mathcal{T}_A$  and thus the travel time  $t_a(x_a)$ . An equilibrium is reached when no driver is able to reduce its travel cost by changing route unilaterally.

**Definition 2.** (Wardrop User Equilibrium [29]) A flow  $f^*$  is called a *Wardrop user equilibrium* if and only if for each OD pair, all paths used by GVs (EVs) have the same travel cost that is no greater than the cost of any unused paths, i.e.

$$0 \leq f_{kg}^{rs*} \perp (c_{kg}^{rs*} - u_g^{rs*}) \geq 0, \forall k \in \mathcal{K}_g^{rs}, \forall rs \quad (10)$$

$$0 \leq f_{ke}^{rs*} \perp (c_{ke}^{rs*} - u_e^{rs*}) \geq 0, \forall k \in \mathcal{K}_e^{rs}, \forall rs \quad (11)$$

Take (10) as an example. For any used path  $k \in \mathcal{K}_g^{rs}$ , we have  $f_{kg}^{rs*} > 0$  and that  $c_{kg}^{rs*}$  equals  $u_g^{rs*}$ . For any unused path, we have  $f_{kg}^{rs*} = 0$  and that the travel cost  $c_{kg}^{rs*}$  is larger than or equal to  $u_g^{rs*}$ . The value of  $u_g^{rs*}$  represents the minimum travel cost that is the same across all used paths from  $r$  to  $s$ . As one driver's driving behavior may influence other drivers' travel time and travel cost, all drivers constitute a Nash game.

### C. Nested Game of Coupled Systems

In Sections II-A and II-B, we introduced the generalized Nash game in the power system and the Nash game in the transportation system, respectively. Externally, the power and transportation systems couple in two ways:

1) The charging demand in the transportation system is part of the electric load in the power system

$$D_i^T = \sum_{c \in C(i)} x_a E_b, \quad a \text{ is the link where CS } c \text{ locates} \quad (12)$$

2) The electricity price  $\gamma_a^c$  on each CS  $c$  equals the sharing price  $\lambda_i$  at node  $i \in \mathcal{E}_N$  if  $c \in C(i)$ . Since each prosumer node can choose to sell energy in the sharing market or serve the transportation system, to prevent arbitrage, the prices for both options should be equal.

The interactions inside and between the two systems are shown in Fig. 3, which is a nested game. To be specific, in the power system, there is a generalized Nash game among all prosumers participating in the energy sharing market. In

the transportation system, all drivers strategically choose their route and play a Nash game. Moreover, the traffic flow in the transportation system will influence the demand in the power system, and the electricity price in the power system will impact the cost of EVs in the transportation system. Therefore, there is a Nash game between two systems.

## III. SOLUTION METHODOLOGY

According to the above analysis, there is a nested game between the coupled power and transportation systems. To the best of our knowledge, there is no existing method to analyze the equilibrium of such a nested game due to its high complexity. To tackle this problem, in this section, we first provide two equivalent optimization models for computing the equilibrium of each system, respectively, with theoretical proofs. Then we turn the external Nash game between the two systems into a MILP based on optimality conditions and linearization techniques, so that we can solve it efficiently.

### A. Optimization Models For Computing the Equilibrium

We first provide two optimization models for computing the equilibrium inside the power and transportation systems, respectively, as stated in Propositions 1 and 2.

**Proposition 1.** The generalized Nash equilibrium  $(b^*, d^*, \lambda^*)$  of the energy sharing game (1) and (3) can be obtained by

$$\min_{d_i, \forall i \in \mathcal{E}_N} \sum_{i \in \mathcal{E}_N} -U_i(d_i) \quad (13a)$$

$$\text{s.t. } p_i + q_i = d_i + d_i^f + D_i^T, i \in \mathcal{E}_N : \xi_i \quad (13b)$$

$$\underline{D}_i \leq d_i \leq \overline{D}_i, \forall i \in \mathcal{E}_N : \psi_{i,d}^\pm \quad (13c)$$

$$q \in \mathcal{F}_c \quad (13d)$$

and  $d_i^*, \forall i \in \mathcal{E}_N$  is unique with  $\lambda_i^* = \xi_i^*$ .

**Proposition 2.** The traffic flow  $f^*$  under Wardrop User Equilibrium can be obtained by

$$\min_{x_a, f_{kg}^{rs}, f_{ke}^{rs}} \sum_{a \in \mathcal{T}_A} \int_0^{x_a} \omega t_a(\theta) d\theta + \sum_{a \in \mathcal{T}_A^C} \gamma_a^c E_b x_a \quad (14a)$$

$$\text{s.t. } x_a = \sum_{rs} \sum_{k \in \mathcal{K}_g^{rs}} f_{kg}^{rs} \delta_{akg}^{rs} + \sum_{rs} \sum_{k \in \mathcal{K}_e^{rs}} f_{ke}^{rs} \delta_{ake}^{rs}, \forall a \quad (14b)$$

$$f_{kg}^{rs} \geq 0, \forall k \in \mathcal{K}_g^{rs}, \forall rs \quad (14c)$$

$$f_{ke}^{rs} \geq 0, \forall k \in \mathcal{K}_e^{rs}, \forall rs \quad (14d)$$

$$\sum_{k \in \mathcal{K}_g^{rs}} f_{kg}^{rs} = q_g^{rs}, \forall rs : u_g^{rs} \quad (14e)$$

$$\sum_{k \in \mathcal{K}_e^{rs}} f_{ke}^{rs} = q_e^{rs}, \forall rs : u_e^{rs} \quad (14f)$$

and  $x_a^*, \forall a \in \mathcal{T}_a$  is unique,  $u_g^{rs*}$  ( $u_e^{rs*}$ ) equals the value of the dual variable of (14e) ((14f)) at optimum.

The proofs of Propositions 1 and 2 are in Appendices A and B, respectively. They facilitate our further analysis.

### B. Transformation and Linearization

Two equivalent optimization models (13) and (14) are derived for computing the equilibrium in the power and transportation systems, respectively. As we can see from Fig.

3, there is a Nash game between the two systems since the electricity price affects the travel cost in the transportation system and the traffic flow affects the demand in the distribution power system. In the following, we convert the optimization problems (13)-(14) into a set of mixed-integer linear constraints by optimality conditions and linearizations, based on which we can obtain the nested game equilibrium of the coupled power and transportation systems.

Regarding the energy sharing problem (13), though the second-order cone constraint (2d) exhibits convexity, its non-linearity still presents a challenge for efficient computation. To address this, polyhedral approximation is applied to turn (2d) into a set of linear constraints. Further, we replace the problem with its primal-dual optimality condition, which is different from the traditional method that is based on the KKT condition. This is because the energy sharing problem comprises mainly inequality constraints and the KKT condition would result in numerous complementarity slackness constraints and require a lot of binary variables to turn it into a solvable form. The primal-dual condition can avoid the high computational burden of KKT since it requires no binary variable. In contrast, the transportation problem (14) mainly comprises of equality constraints that can be efficiently replaced by its KKT condition.

1) *Primal-dual Condition of Power System Problem (13)*: The polyhedral approximation technique in [30] is employed to approximate the nonlinear constraint (2d) with linear constraints. First, constraint (2d) is rewritten as

$$\sqrt{(2P_{ni})^2 + (2Q_{ni})^2 + (\ell_{ni} - v_n)^2} \leq \ell_{ni} + v_n, \forall (n, i) \in \mathcal{E}_L, \quad (15)$$

which is further equivalently split into two second-order cones

$$\sqrt{(2P_{ni})^2 + (2Q_{ni})^2} \leq W_{ni}, \forall (n, i) \in \mathcal{E}_L, \quad (16a)$$

$$\sqrt{W_{ni}^2 + (\ell_{ni} - v_n)^2} \leq \ell_{ni} + v_n, \forall (n, i) \in \mathcal{E}_L. \quad (16b)$$

Then, each constraint in the form of  $\sqrt{x_1^2 + x_2^2} \leq x_3$  is approximated by a series of linear equalities and inequalities.

$$\begin{cases} \xi^0 \geq |x_1| \\ \eta^0 \geq |x_2| \end{cases}, \quad \begin{cases} \xi^Z \leq x_3 \\ \eta^Z \leq \tan\left(\frac{\pi}{2^{Z+1}}\right)\xi^Z \end{cases} \\ \begin{cases} \xi^z = \cos\left(\frac{\pi}{2^{z+1}}\right)\xi^{z-1} + \sin\left(\frac{\pi}{2^{z+1}}\right)\eta^{z-1} \\ \eta^z \geq \left| -\sin\left(\frac{\pi}{2^{z+1}}\right)\xi^{z-1} + \cos\left(\frac{\pi}{2^{z+1}}\right)\eta^{z-1} \right| \end{cases}, \quad z = 1, \dots, Z \end{cases} \quad (17)$$

where  $\xi^z, \eta^z, \forall z = 0, 1, 2, \dots, Z$ , are auxiliary variables. The approximation error can be adjusted by manipulating the parameter  $Z$ . Finally, we use (17) to replace the nonlinear constraint (2d). The convex objective function  $-U_i(d_i), \forall i$  can also be linearized via a convex combination approach [31]. Then, we get a LP-based energy sharing problem.

So far, the energy sharing game problem (13) can be cast as a compact form

$$\min_y c_m^T y_v, \text{ s.t. } A_1 y_v = D_{TS} : \lambda_v, A_2 y_v \geq B_2 : \mu_v \quad (18)$$

where vector  $y_v$  includes physical variables such as  $q_i, Q_i, P_{ni}, Q_{ni}, v_i, \ell_{ni}, d_i$  and auxiliary variables  $\xi^k, \eta^k$ , and the matrices  $c_m, A_1, A_2, D_{TS}$  and  $B_2$  are constant coefficients. Vector  $D_{TS}$  collects the transportation power demand  $D_i^T$  of all prosumers.  $\lambda_v$  is the dual variable associated with  $A_1 y_v = D_{TS}$  and its  $j$ -th entry is the sharing price of prosumer  $j$ . All other equality and inequality constraints are included in  $A_2 y_v \geq B_2$  with a dual variable vector  $\mu_v$ . Then, we can obtain the primal-dual condition

$$A_1 y_v = D_{TS}, A_2 y_v \geq B_2 \quad (19a)$$

$$A_1^T \lambda_v + A_2^T \mu_v = c_m, \mu_v \geq 0 \quad (19b)$$

$$c_m^T y_v = \lambda_v^T D_{TS} + \mu_v^T B_2 \quad (19c)$$

The primal and dual constraints are represented by equations (19a) and (19b), respectively. Due to the strong duality that always holds for LP, we have (19c), i.e., the objective values of the primal and dual problems are equal.

2) *KKT Condition of Problem (14)*: The KKT condition is

$$(5), (8), (9), (10), (11) \quad (20)$$

For the above KKT condition (20), nonlinearity lies in the complementary slackness condition and the travel time  $t_a(x_a)$ . The complementary slackness condition in the form of  $0 \leq x \perp y \geq 0$  can be linearized using the Big-M method.

3) *Linearization of the Bilinear Term and Travel Time.*:

When combing the conditions (19) and (20), the presence of the bilinear product term  $\lambda_v^T D_{TS}$  on the right-hand side of (19c), where  $D_{TS}$  is a linear expression of  $x_a$ , makes the problem nonlinear again. Such a term is approximated and convexified by McCormick envelope [32]. To enhance the accuracy of the approximation, here we adopt the piecewise McCormick envelope, which leads to tighter boundaries. The bilinear term is replaced by a new variable  $\sigma$ . Let  $\lambda_v^{\min}$  and  $\lambda_v^{\max}$  represent the lower and upper bounds of variable  $\lambda_v$ .  $|S|$  is the partition number and  $s$  is partition index. Binary variable  $y_s = 1$  means  $\lambda_{v,s}$  belong to this disjunction; otherwise,  $y_s = 0$ .  $D_{TS}$  is also partitioned as  $D_{TS,s}, \forall s \in S$ .

$$\sigma \geq \sum_{s=1}^{|S|} (D_{TS}^{\min} \lambda_{v,s} + \lambda_{v,s}^{\min} D_{TS,s} - D_{TS}^{\min} \lambda_{v,s}^{\min} y_s), \forall s \in S \quad (21a)$$

$$\sigma \geq \sum_{s=1}^{|S|} (D_{TS}^{\max} \lambda_{v,s} + \lambda_{v,s}^{\max} D_{TS,s} - D_{TS}^{\max} \lambda_{v,s}^{\max} y_s), \forall s \in S \quad (21b)$$

$$\sigma \leq \sum_{s=1}^{|S|} (D_{TS}^{\max} \lambda_{v,s} + \lambda_{v,s}^{\min} D_{TS,s} - D_{TS}^{\max} \lambda_{v,s}^{\min} y_s), \forall s \in S \quad (21c)$$

$$\sigma \leq \sum_{s=1}^{|S|} (D_{TS}^{\min} \lambda_{v,s} + \lambda_{v,s}^{\max} D_{TS,s} - D_{TS}^{\min} \lambda_{v,s}^{\max} y_s), \forall s \in S \quad (21d)$$

$$\lambda_v = \sum_{s=1}^{|S|} \lambda_{v,s}, D_{TS} = \sum_{s=1}^{|S|} D_{TS,s}, \sum_{s=1}^{|S|} y_s = 1, \forall s \in S \quad (21e)$$

$$\lambda_{v,s}^{\min} = \lambda_v^{\min} + (\lambda_v^{\max} - \lambda_v^{\min})(s-1)/|S|, \forall s \in S \quad (21f)$$

$$\lambda_{v,s}^{\max} = \lambda_v^{\max} - (\lambda_v^{\max} - \lambda_v^{\min})s/|S|, \forall s \in S \quad (21g)$$

$$\lambda_{v,s}^{\min} y_s \leq \lambda_{v,s} \leq \lambda_{v,s}^{\max} y_s, \forall s \in S \quad (21h)$$

$$D_{TS,s}^{\min} y_s \leq D_{TS,s} \leq D_{TS,s}^{\max} y_s, \forall s \in S \quad (21i)$$

$$y_s \in \{0, 1\}, \forall s \in S \quad (21j)$$

After above transformation, the only nonlinear terms exist in travel time  $t_a(x_a)$ , i.e., (6) and (7). In this paper, we perform

piecewise linear approximation by using SOS2 variables [33], which is a vector of variables with at most two adjacent elements being able to take nonzero values. The specific processes are omitted for brevity. After the above transformation based on optimality conditions and the linearization techniques, the equilibrium of the nested game in Fig. 3 can be calculated by solving a MILP.

#### IV. CASE STUDIES

Numerical experiments are carried out to validate the proposed method and propositions. All simulations are implemented in MATLAB, solved by Gurobi, and run on a laptop with an Intel Core i7 1.80 GHz CPU and 16 GB RAM.

##### A. System Setup

A modified IEEE 33-bus system is adopted as the power network as shown in Fig. 4. We first consider the case with four prosumers located at buses 10, 18, 23, and 30, respectively. Each prosumer possesses renewable generation ( $p_1/p_2/p_3/p_4=3/1/4/2\text{MW}$ ), fixed load ( $d_1/d_2/d_3/d_4=0.1/0.2/0.15/0.1\text{MW}$ ), adjustable load, and powers one or multiple charging stations (CSs). The upper and lower limits of voltage magnitudes for each bus are 1.06 p.u. and 0.94 p.u., respectively. Fig. 5 (left) shows the transportation network (TN) with 12 nodes and 20 links. The parameters of each link can be found in [32]. The OD pairs and trip rates are listed in TABLE I. The base value of traffic flow is 100 vehicles/hour and we assume that EVs account for 5% of the trip rate of each OD pair. As discussed in Section II-B, bypass links are added to facilitate the analysis. As a result, it is expanded to a 28-node and 44-link network, as shown in Fig. 5 (right). Based on the expanded transportation network, we then build its node-link incidence matrix and enumerate the paths for GV and EV between OD pair  $(r,s)$  using the method in [26]. Regarding the coupling between power and transportation networks, we assume CS1 and CS2 are powered by prosumer 1, CS3 and CS4 by prosumer 2, CS5 and CS6 by prosumer 3, and CS7 and CS8 by prosumer 4. Each EV's charging demand is assumed to be  $E_b = 20\text{kWh}$  and charging time is  $t_{a,\mu}^c = 20\text{min}$ . The monetary cost of travel time is  $\omega = 10\text{\$/hr}$ .

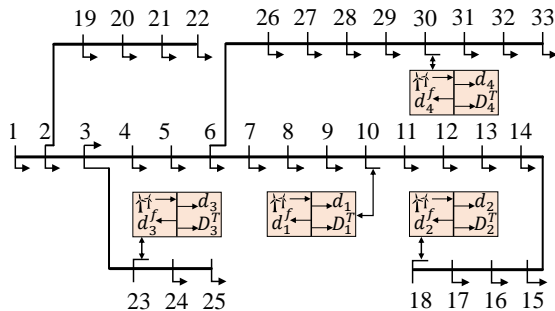


Fig. 4. Modified IEEE 33-bus test system with 4 prosumers.

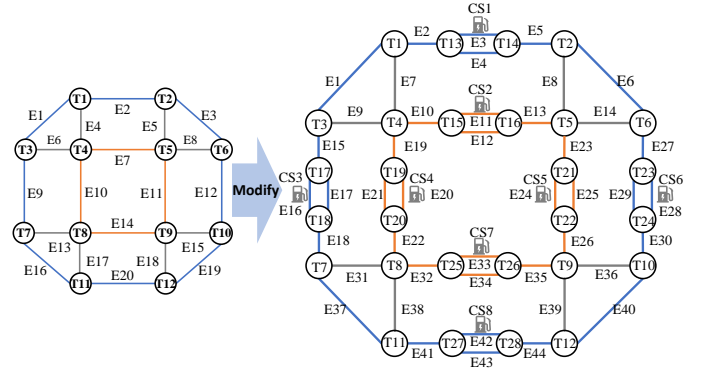


Fig. 5. Left: Original transportation network with 12 nodes and 20 links. Right: Expanded transportation network with 28 nodes and 44 links.

TABLE I  
OD PAIRS AND THEIR TRIP RATES (IN P.U., 1P.U.=100 VEHICLES/H).

OD pair	$q_{rs}$						
T1-T6	5	T1-T10	15	T1-T12	10	T1-T11	5
T3-T6	5	T3-T10	15	T3-T12	15	T3-T11	5
T4-T9	10	T4-T10	10	T4-T12	5		

##### B. Equilibrium Results

The equilibrium of the external Nash game between the power and transportation systems is characterized by the sharing/charging price  $\lambda_i^*$  and traffic flow  $x_q^*$ . Moreover, they are the results of the two internal (generalized) Nash equilibria. At the equilibrium, we compute the difference between the left-hand side and the right-hand side of (15) under  $Z = 6$ . The errors associated with each line fall within the range of  $-0.85 \times 10^{-3}$  to  $2.18 \times 10^{-3}$ , indicating that the proposed polyhedral approximation can achieve desirable accuracy. The computation takes 120 seconds.

We first discuss the energy sharing equilibrium in the power network. At the equilibrium point, the power distribution within each prosumer is shown in Fig. 6. All sharing quantity  $q_i < 0, \forall i$ , indicating that the four prosumers 1-4 are all sellers in the energy market. The sum of  $|q_1|$  to  $|q_4|$  corresponds to the injected power into the power network for serving the loads located at other buses and compensating for the power loss in the AC distribution network. The energy sharing price of each prosumer is  $\lambda_1 = 0.4336\text{\$/kWh}$ ,  $\lambda_2 = 0.4402\text{\$/kWh}$ ,  $\lambda_3 = 0.4342\text{\$/kWh}$ , and  $\lambda_4 = 0.4400\text{\$/kWh}$ . The prices determined by energy sharing are also used as the EV charging prices in the transportation system. Owing to the difference in charging prices, it can be seen that prosumers with lower prices will serve a larger EV charging load and vice versa. For instance, prosumer 1 serves the largest EV charging load of 4.5975 MWh because it offers the lowest charging price of 0.4336  $\text{\$/kWh}$ .

As for the Nash game in the transportation system, the equilibrium is reached when (14) is met. Fig. 7 depicts the traffic flows of GV and EV across each expanded TN link. As seen, GV solely utilize regular and bypass links and the traffic flow of EV is distributed across all three types of links. To demonstrate the reached equilibrium, we take OD

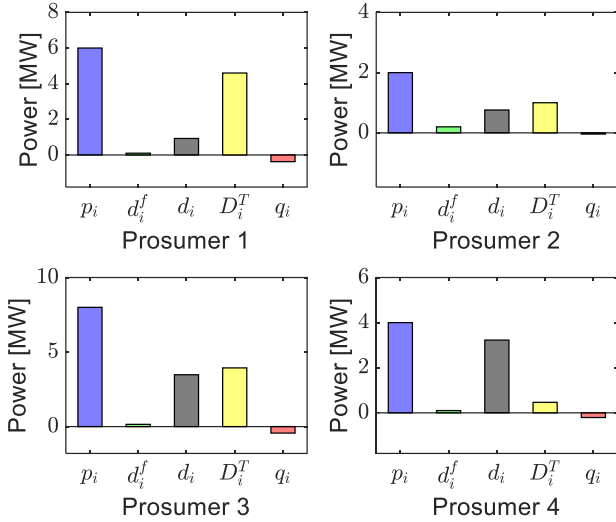


Fig. 6. Power distribution within each prosumer.

pair T1-T12 for example. Under the UE, for OD pair T1-T12, all EVs select the most cost-effective path (E2-E3-E5-E6-E27-E29-E30-E40), with a travel cost of 19.45\$, including a travel time cost of 10.78\$ and a charging cost of 8.67\$. On the contrary, if an EV selects the path (E7-E10-E11-E13-E23-E25-E26-E39), the corresponding travel cost would be 25.57\$. This cost comprises a travel time cost of 16.9\$ and a charging cost of 8.67\$. The two paths have the same charging cost because both CS1 and CS2 are powered by the same prosumer 1, but different travel cost. The second path is more expensive than the first one that is the optimal. However, for GV's traveling between the OD pair T1-T12, there are two optimal paths. The first path involves passing (E2-E4-E5-E6-E27-E29-E30-E40) and the second path traverses (E1-E15-E17-E18-E37-E41-E43-E44). Both of them have the same travel cost of 7.41\$. Notably, their respective costs are less than those associated with the non-selected routes such as the path (E7-E10-E12-E13-E23-E25-E26-E39), which requires 13.43\$. These results align with the definition of Wardrop UE.

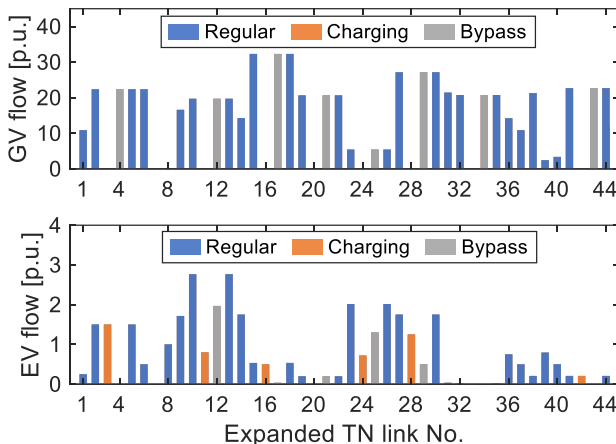


Fig. 7. GV and EV traffic flow assignment in each expanded TN link.

### C. Distributed Energy Sharing Mechanism Verification

Proposition 1 states that the GNE of energy sharing game (1) and (3) can be obtained by solving the centralized problem (13). To verify Proposition 1, we first fix the transportation power demand  $D_i^T$  of each prosumer and solely solve the centralized counterpart problem (13). Under this setting, we can obtain prosumers' elastic loads:  $d_1 = 0.93\text{MW}$ ,  $d_2 = 0.75\text{MW}$ ,  $d_3 = 3.47\text{MW}$ ,  $d_4 = 3.23\text{MW}$ , and their sharing prices by retrieving the dual variables of (13a) with Gurobi:  $\lambda_1 = 0.41\$/\text{kWh}$ ,  $\lambda_2 = 0.42\$/\text{kWh}$ ,  $\lambda_3 = 0.43\$/\text{kWh}$ ,  $\lambda_4 = 0.44\$/\text{kWh}$ . The prices are slightly different from those mentioned previously because of the linearization and approximation errors. Then, we let the market operator and prosumers play the generalized Nash game in a distributed way according to (1) and (3). The changes of energy sharing prices and elastic demands are illustrated in Fig. 8. As the iteration proceeds, we can see that both the energy sharing prices and prosumers' strategies of load adjustment amount gradually converge. At GNE, we have  $d_1 = 0.91\text{MW}$ ,  $d_2 = 0.77\text{MW}$ ,  $d_3 = 3.49\text{MW}$ ,  $d_4 = 3.22\text{MW}$ , and  $\lambda_1 = 0.41\$/\text{kWh}$ ,  $\lambda_2 = 0.42\$/\text{kWh}$ ,  $\lambda_3 = 0.43\$/\text{kWh}$ ,  $\lambda_4 = 0.44\$/\text{kWh}$ . They are almost the same as the centralized solution. Therefore, Proposition 1 is verified.

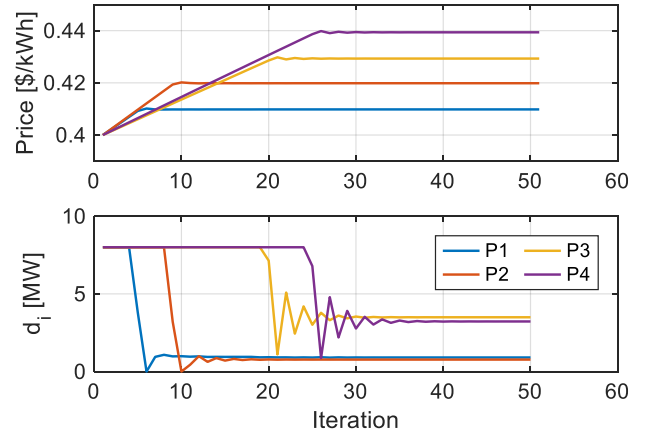


Fig. 8. Market sharing prices and optimal strategies of four prosumers. "P" is the abbreviation of prosumer.

### D. Performance Comparison

To demonstrate the advantage of the proposed approach, three benchmarks used in the literature are conducted and compared with the proposed method.

- Benchmark 1 (B1): Best response decomposition method [26]. It attempts to iteratively solve the energy sharing problem of power network with fixed transportation power demand and then uses the clearing price to solve the traffic flow assignment problem until convergence. However, this method may or may not converge.
- Benchmark 2 (B2): Traditional KKT conditions method. Both energy sharing equilibrium and the Wardrop user equilibrium are replaced with their KKT conditions.
- Benchmark 3 (B3): Partial energy sharing. We assume some prosumers do not participate in energy sharing but

operate in a self-sufficiency mode, i.e.,  $q_i = 0$ . Other settings are the same as the proposed method.

- Proposed method: All prosumers participate in energy sharing and we solve the nested game via the derived MILP without iteration.

For B1, in our test, if we keep the power network constraints (e.g., bus voltage limits and line flow limits) the same as those used in the proposed method, B1 stops after 1 iteration because infeasibility occurs when solving the power system problem. Then, we enlarge the bus voltage and line flow limits' interval. However, B1 still fails to converge and oscillation occurs on the transportation power demand  $D_i^T$  and sharing prices  $\lambda_i$  as shown in Fig. 9. For example, based on the outcomes of  $D_i^T$  at iteration 2 where  $D_1^T > D_2^T > D_3^T > D_4^T$ , iteration 3 first clears the power market with  $\lambda_1^T = 1.76\$/\text{kWh}$ ,  $\lambda_2^T = 4.56\$/\text{kWh}$ ,  $\lambda_3^T = 0.43\$/\text{kWh}$ ,  $\lambda_4^T = 0.44\$/\text{kWh}$ . The resulting price changes cause the change of EVs' routing in the transportation system, which gives  $D_3^T > D_4^T > D_1^T = D_2^T$ . As a result, at iteration 4, the sharing prices return to its previous values, leading to oscillation. For B2, the computational complexity becomes a challenge as the KKT conditions of the energy sharing problem produce numerous complementarity slackness constraints and require a lot of binary variables to yield a solvable form. Simulation shows it cannot give a result in 1 hour, the target time interval of this studied problem. Our proposed method solves the MILP without iterations and does not have a convergence problem. TABLE II summarizes the utility/cost of power system (PS) and transportation system (TS) under B3 and the proposed method. In B3, prosumer 4 does not participate in energy sharing. From the table, we can find that the proposed method has a better utility (cost) of PS (TS) than B3. It indicates the positive influence of energy sharing on the joint operation of power and transportation system.

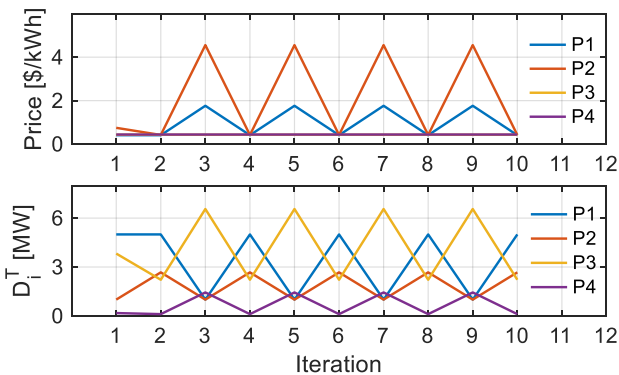


Fig. 9. The oscillation of  $D_i^T$  and  $\lambda_i$  under B1.

TABLE II  
COST COMPARISON BETWEEN DIFFERENT METHODS (UNIT:\$).

	Utility of PS $\sum_i U_i(d_i)$	Cost of TS $\sum_{a \in T_A} [\omega t_a x_{ag} + (\gamma_a^c E_b + \omega t_a) x_{ae}]$
B3	3561.86	124743.91
Proposed	3613.77	124619.38

We further compare the  $\lambda_i$  and  $D_i^T$  under B3 and the proposed method because the EVs' choice of CS is closely

related to their offered charging prices. Compared with B3, the sharing price difference between prosumer 3 and 4 under the proposed method is larger. This difference incentivizes some EVs to change their original routes determined by B3, and more EVs select charging stations operated by prosumer 3 that offers a relatively lower price, as shown in Fig. 10. For example, for OD pair T4-T10, the proposed method's solution allocates all trip rate (0.5p.u.) to pass through E10-E12-E13-E14-E27-E28(prosumer 3)-E30. On the contrary, B3 dispatches a smaller EV trip rate (0.375p.u.) to go through that path and dispatch the remaining EV trip rate (0.125p.u.) to go through path E19-E21-E22-E32-E33(prosumer 4)-E35-E36 because of the close prices of prosumers 3 and 4. This comparison suggests that energy sharing affects the EV traffic flow on the transportation system through pricing.

TABLE III  
SHARING PRICES OF B3 AND PROPOSED METHOD (UNIT: \$/KWH).

Prosumer	1	2	3	4
B3	0.4392	0.4442	0.4431	0.4432
Proposed	0.4336	0.4402	0.4342	0.4400

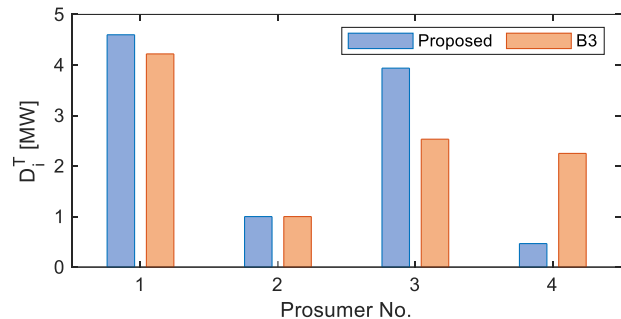


Fig. 10. Illustration of the traffic flow of OD pair T1-T12 in B3 and the proposed method.

### E. 8-Prosumer System

The case studies and analyses above have demonstrated the effectiveness of the proposed method. Here, we increase the number of prosumers in the distribution network to 8 (Fig. 4), with each prosumer serving one CS in the transportation system (Fig. 5). Fig. 11 shows the renewable generation and energy sharing amounts of each prosumer. In this energy sharing market, prosumers 1 and 6 become buyers and others are sellers, the roles of which are more diverse than the 4-prosumer system.

The determined sharing prices are illustrated in Fig. 12. As shown, the sharing prices vary from 0.41 to 0.46\$/kWh. The lower prices appear in prosumers 1 and 7, which operate charging stations 1 and 7, respectively. Correspondingly, we can see in Fig. 13 that the charging load of charging stations 1 and 7 are the highest. It reflects the impact of the sharing price on the EV routing. In addition, the computation time to solve this 8-prosumer case is 710s under the piecewise McCormick envelop of  $|S| = 3$ , which is higher than the 4-prosumer system but is still acceptable.

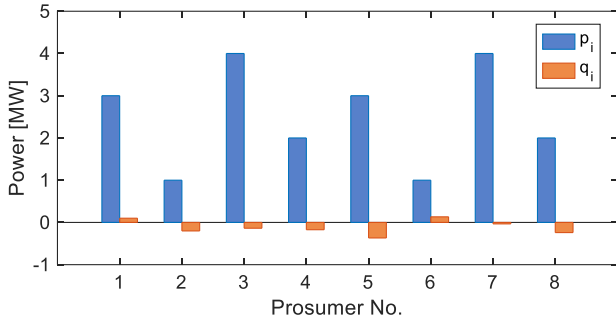


Fig. 11. Energy production and sharing amount outcome of 8 prosumers.

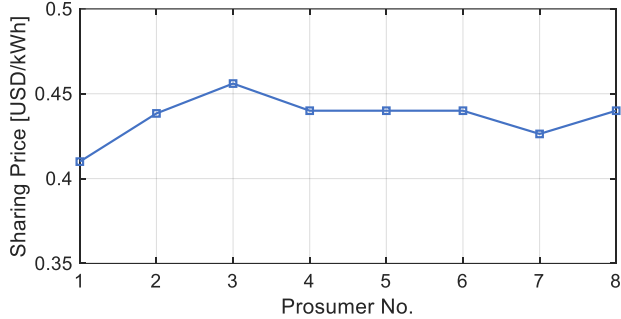


Fig. 12. Sharing prices outcome of 8 prosumers.

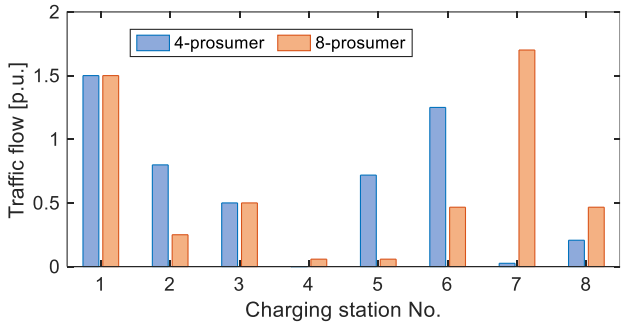


Fig. 13. Traffic flow distribution of 4-prosumer and 8-prosumer system.

### F. Impact of Parameters

#### 1) Partition Number of Piecewise McCormick Envelope:

In this paper, the piecewise McCormick envelope technique is used to approximate the bilinear term. To investigate the impact of partition number  $|S|$  on the accuracy, we change  $|S|$  from 5 to 20. We calculate the error between the approximation value  $\sigma$  in (21) and the actual product of the values  $D_i^T$  and  $\lambda_i$ , as shown in TABLE IV. Generally, a larger number of partitions used in the piecewise McCormick envelope generates a more accurate result. When  $|S| = 10$ , the error has fallen within 5%. As  $|S|$  increases, the solving time increases significantly due to using more binary variables. Therefore, the choice of partition number depends on the trade-off between solution accuracy and computational efficiency.

2) *EV Charging Demand*: Fig. 14 shows the impact of EV charging demand per car  $E_b$  on the utility/cost of PS and TS. As the EV charging demand increases, the utility of PS decreases. This is because more electricity is required

TABLE IV  
THE APPROXIMATION ERROR AND SOLVING TIME UNDER DIFFERENT PARTITIONS.

Prosumer No.	1	2	3	4	
$ S =5$	error	4%	18.18%	0.83%	18.18%
	solver time	80s			
$ S =8$	error	1%	16.14%	16.28%	2.45%
	solver time	104s			
$ S =10$	error	1.49%	0.20%	1.33%	0%
	solver time	120s			
$ S =20$	error	0.38%	2.91%	2.33%	2.08%
	solver time	1644s			

by the charging load, so less flexible load can be supplied and their utility decreases. In addition, as the EV charging demand increases, the cost of TS is not significantly affected. This indicates that EV charging demand has a major impact on the power system, while its influence on the transportation system is relatively small.

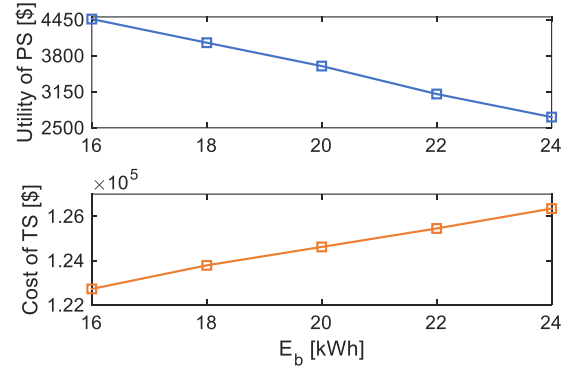


Fig. 14. Impact of  $E_b$  on the utility/cost of PS and TS.

3) *Time Monetary Value*: Fig. 15 depicts the impact of the time monetary value  $\omega$  on the utility/cost of PS and TS. As  $\omega$  increases, the cost of TS significantly rises from  $1.02 \times 10^5$  to  $1.36 \times 10^5$ , representing an increase of 33%. In contrast, the utility of PS varies within a relatively narrow range of 3564\$ and 3614\$. This implies that the parameter  $\omega$  mainly affects the transportation system and has little effect on power system.

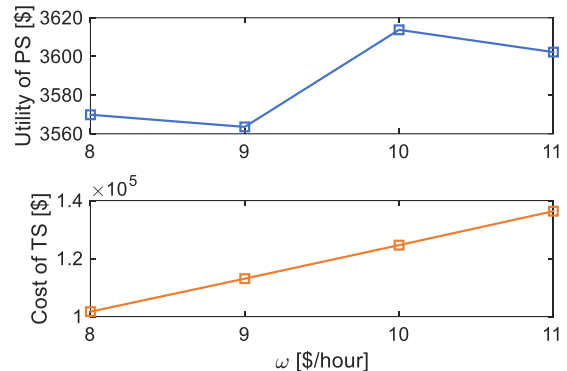


Fig. 15. Utility/cost of PS and TS under different  $\omega$ .

## V. CONCLUSION

This paper presents a novel nested game model to characterize the complex interaction between transportation and power system. In the power system, we propose an energy sharing mechanism for prosumers, which casts down to a generalized Nash game. In the transportation system, all drivers strategically choose their routes with the goal of minimizing their travel costs, resulting in a Nash game. Externally, the two systems constitute a Nash game. To analyze the equilibrium of this nested game, two equivalent models are provided. Then optimality conditions and linearization techniques are employed to convert the nested game model into a MILP, enabling efficient computation. Case studies demonstrate the effectiveness and benefits of the proposed method. We have the following findings: 1) The EV routing to charging stations is closely related to their offering prices. 2) Prosumers engaging in energy sharing can reduce the operation costs of both systems. 3) The proposed method can greatly reduce the computational time and avoid the non-convergence issue of the traditional best response decomposition method.

## REFERENCES

- [1] L. Kong, H. Zhang, W. Li, H. Bai, and N. Dai, "Spatial-temporal scheduling of electric bus fleet in power-transportation coupled network," *IEEE Trans. Transport. Electric.*, vol. 9, no. 2, pp. 2969–2982, 2023.
- [2] J. Hamilton, B. Walton, J. Ringrow, G. Alberts, S. Fullerton-Smith, and E. Day, "Electric vehicles: Setting a course for 2030," *Deloitte Insights*, 2020.
- [3] "2017 distributed wind market report," Office of Energy Efficiency & Renewable Energy, Tech. Rep., 2017.
- [4] S. Agnew and P. Dargusch, "Effect of residential solar and storage on centralized electricity supply systems," *Nature Climate Change*, vol. 5, no. 4, p. 315, 2015.
- [5] Y. Parag and B. K. Sovacool, "Electricity market design for the prosumer era," *Nature Energy*, vol. 1, no. 4, pp. 1–6, 2016.
- [6] W. Tushar, T. K. Saha, C. Yuen, D. Smith, and H. V. Poor, "Peer-to-peer trading in electricity networks: An overview," *IEEE Trans. Smart Grid*, vol. 11, no. 4, pp. 3185–3200, 2020.
- [7] C. Lyu, Y. Jia, and Z. Xu, "Fully decentralized peer-to-peer energy sharing framework for smart buildings with local battery system and aggregated electric vehicles," *Appl. Energy*, vol. 299, p. 117243, 2021.
- [8] C. Long, Y. Zhou, and J. Wu, "A game theoretic approach for peer to peer energy trading," *Energy Procedia*, vol. 159, pp. 454–459, 2019.
- [9] L. Han, T. Morstyn, and M. McCulloch, "Incentivizing prosumer coalitions with energy management using cooperative game theory," *IEEE Trans. Power Syst.*, vol. 34, no. 1, pp. 303–313, 2018.
- [10] S. Cui, Y.-W. Wang, Y. Shi, and J.-W. Xiao, "Community energy cooperation with the presence of cheating behaviors," *IEEE Trans. Smart Grid*, vol. 12, no. 1, pp. 561–573, 2020.
- [11] N. Liu, X. Yu, C. Wang, and J. Wang, "Energy sharing management for microgrids with PV prosumers: A Stackelberg game approach," *IEEE Trans. Ind. Informat.*, vol. 13, no. 3, pp. 1088–1098, 2017.
- [12] N. Liu, X. Yu, C. Wang, C. Li, L. Ma, and J. Lei, "Energy-sharing model with price-based demand response for microgrids of peer-to-peer prosumers," *IEEE Trans. Power Syst.*, vol. 32, no. 5, pp. 3569–3583, 2017.
- [13] X. Xu, Y. Xu, M.-H. Wang, J. Li, Z. Xu, S. Chai, and Y. He, "Data-driven game-based pricing for sharing rooftop photovoltaic generation and energy storage in the residential building cluster under uncertainties," *IEEE Trans. Ind. Informat.*, vol. 17, no. 7, pp. 4480–4491, 2020.
- [14] Y. Chen, C. Zhao, S. H. Low, and S. Mei, "Approaching prosumer social optimum via energy sharing with proof of convergence," *IEEE Trans. Smart Grid*, vol. 12, no. 3, pp. 2484–2495, 2020.
- [15] H. Le Cadre, P. Jacquot, C. Wan, and C. Alasseur, "Peer-to-peer electricity market analysis: From variational to generalized nash equilibrium," *European J. Operational Research*, vol. 282, no. 2, pp. 753–771, 2020.
- [16] Y. Chen, C. Zhao, S. H. Low, and A. Wierman, "An energy sharing mechanism considering network constraints and market power limitation," *IEEE Trans. Smart Grid*, 2023.
- [17] H. Zhang, Z. Hu, and Y. Song, "Power and transport nexus: Routing electric vehicles to promote renewable power integration," *IEEE Trans. Smart Grid*, vol. 11, no. 4, pp. 3291–3301, 2020.
- [18] W. Tang and Y. J. Zhang, "A model predictive control approach for low-complexity electric vehicle charging scheduling: Optimality and scalability," *IEEE Trans. Power Syst.*, vol. 32, no. 2, pp. 1050–1063, 2016.
- [19] H. Zhang, S. J. Moura, Z. Hu, W. Qi, and Y. Song, "Joint pev charging network and distributed pv generation planning based on accelerated generalized benders decomposition," *IEEE Trans. Transport. Electric.*, vol. 4, no. 3, pp. 789–803, 2018.
- [20] W. Wei, S. Mei, L. Wu, M. Shahidehpour, and Y. Fang, "Optimal traffic-power flow in urban electrified transportation networks," *IEEE Trans. Smart Grid*, vol. 8, no. 1, pp. 84–95, 2016.
- [21] S. Lv, Z. Wei, G. Sun, S. Chen, and H. Zang, "Optimal power and semi-dynamic traffic flow in urban electrified transportation networks," *IEEE Trans. Smart Grid*, vol. 11, no. 3, pp. 1854–1865, 2019.
- [22] Y. Sun, Z. Chen, Z. Li, W. Tian, and M. Shahidehpour, "Ev charging schedule in coupled constrained networks of transportation and power system," *IEEE Trans. Smart Grid*, vol. 10, no. 5, pp. 4706–4716, 2018.
- [23] W. Wei, L. Wu, J. Wang, and S. Mei, "Expansion planning of urban electrified transportation networks: A mixed-integer convex programming approach," *IEEE Trans. Transport. Electric.*, vol. 3, no. 1, pp. 210–224, 2017.
- [24] X. Wang, M. Shahidehpour, C. Jiang, and Z. Li, "Resilience enhancement strategies for power distribution network coupled with urban transportation system," *IEEE Trans. Smart Grid*, vol. 10, no. 4, pp. 4068–4079, 2018.
- [25] W. Liu, X. Wang, and Y. Xu, "Bilevel planning of wireless charging lanes in coupled transportation and power distribution networks," *IEEE Trans. Transport. Electric.*, pp. 1–1, 2023.
- [26] W. Wei, L. Wu, J. Wang, and S. Mei, "Network equilibrium of coupled transportation and power distribution systems," *IEEE Trans. Smart Grid*, vol. 9, no. 6, pp. 6764–6779, 2017.
- [27] F. Facchinei and C. Kanzow, "Generalized Nash equilibrium problems," *Annals of Operations Research*, vol. 175, no. 1, pp. 177–211, 2010.
- [28] U. S. B. of Public Roads, *Traffic assignment manual for application with a large, high speed computer*. US Department of Commerce, Bureau of Public Roads, Office of Planning, Urban Planning Division, 1964.
- [29] J. G. Wardrop, "Road paper. some theoretical aspects of road traffic research," *Proceedings of the institution of civil engineers*, vol. 1, no. 3, pp. 325–362, 1952.
- [30] A. Ben-Tal and A. Nemirovski, "On polyhedral approximations of the second-order cone," *Mathematics of Operations Research*, vol. 26, no. 2, pp. 193–205, 2001.
- [31] L. Wu, "A tighter piecewise linear approximation of quadratic cost curves for unit commitment problems," *IEEE Trans. Power Syst.*, vol. 26, no. 4, pp. 2581–2583, 2011.
- [32] S. Lv, S. Chen, Z. Wei, and H. Zhang, "Power-transportation coordination: Toward a hybrid economic-emission dispatch model," *IEEE Trans. Power Syst.*, vol. 37, no. 5, pp. 3969–3981, 2022.
- [33] E. Beale and J. J. Forrest, "Global optimization using special ordered sets," *Mathematical Programming*, vol. 10, no. 1, pp. 52–69, 1976.

## APPENDIX A

### PROOF OF PROPOSITION 1

Denote  $q_i = -m_a \lambda_i + b_i, \forall i \in \mathcal{E}_N$ . Then problem (1) can be equivalently written as

$$\min_{q_i, \forall i} \sum_{i \in \mathcal{E}_N} (q_i - b_i)^2 \quad (\text{A.1a})$$

$$\text{s.t. } q \in \mathcal{F}_c \quad (\text{A.1b})$$

Suppose  $(b^*, d^*, \lambda^*)$  is the GNE of the energy sharing game (1) and (3), then for problem (1) we have

$$\sum_{i \in \mathcal{E}_N} (q_i - q_i^*)(q_i^* - b_i^*) \geq 0, \forall q \in \mathcal{F}_c \quad (\text{A.2})$$

Let  $\mathcal{D}_i := \{d_i \mid \underline{D}_i \leq d_i \leq \overline{D}_i\}$ . For problem (3), first we substitute (3b) into the objective function (3a) to eliminate  $b_i$ , then for all  $i$  in  $\mathcal{E}_N$  its optimality condition is

$$-U_i(d_i) + U_i(d_i^*) + (d_i - d_i^*)\lambda_i^* \geq 0, \forall d \in \mathcal{D}_i \quad (\text{A.3})$$

For problem (13), its Lagrangian function defined on  $\Omega := \prod_{i \in \mathcal{E}_N} \mathcal{D}_i \times \mathcal{F}_c \times \mathbb{R}^{|\mathcal{E}_N|}$  is

$$L(d, p^{out}, \xi) = \sum_{i \in \mathcal{E}_N} -U_i(d_i) + \sum_{i \in \mathcal{E}_N} \xi_i(d_i + d_i^f + D_i^T - p_i - q_i) \quad (\text{A.4})$$

Let  $(\hat{d}, \hat{q}, \hat{\xi})$  be a saddle point of the Lagrangian function, then  $(\hat{d}, \hat{q}, \hat{\xi}) \in \Omega$  and it satisfies  $\forall (d, q, \xi) \in \Omega$ :

$$\left[ -U_i(d_i) + U_i(\hat{d}_i) + (d_i - \hat{d}_i)\hat{\xi}_i \right] \geq 0, \forall i \in \mathcal{E}_N \quad (\text{A.5a})$$

$$- \sum_{i \in \mathcal{E}_N} (q_i - \hat{q}_i)(\hat{\xi}_i) \geq 0 \quad (\text{A.5b})$$

$$\sum_{i \in \mathcal{E}_N} (\hat{\xi}_i - \hat{\xi}_i)(\hat{d}_i + d_i^f + D_i^T - p_i - \hat{q}_i) \leq 0 \quad (\text{A.5c})$$

**Existence.** If problem (13) is feasible, suppose  $\hat{d}$  is its optimal solution and  $\hat{\xi}$  is the corresponding dual variable. Let  $d^* = \hat{d}$ ,  $\lambda^* = \hat{\xi}$ ,  $q_i^* = \hat{d}_i + d_i^f + D_i^T - p_i$  for all  $i$  in  $\mathcal{E}_N$ , and  $b_i^* = m_a \hat{\xi}_i + q_i^*$ ,  $\forall i \in \mathcal{E}_N$ , then it is easy to check that (A.3) and (A.2) are met. Thus, we have constructed a GNE  $(d^*, b^*, \lambda^*)$ .

**Uniqueness.** Given a GNE  $(d^*, b^*, \lambda^*)$ , we have  $b_i^* = d_i^* + d_i^f + D_i^T - p_i + m_a \lambda_i^*$  for all  $i$  in  $\mathcal{E}_N$ . Let  $\hat{d} = d^*$ ,  $\hat{\xi} = \lambda^*$ , and  $\hat{q} = -m_a \lambda^* + b^*$ , then it is easy to check that  $(\hat{d}, \hat{q}, \hat{\xi})$  satisfies (A.5), so  $\hat{d}$  is the optimal solution of (13) and  $\hat{\xi}$  is the corresponding dual variable. Since the objective function is strictly convex, and the constraint sets  $\mathcal{D}_i, \forall i \in \mathcal{E}_N$  and  $\mathcal{F}_c$  are all closed convex sets, problem (13) has a unique solution, so  $\hat{d}$  is unique and problem (13) is feasible.

## APPENDIX B PROOF OF PROPOSITION 2

The Lagrangian of the equivalent optimization problem (14) with respect to the equality constraints (14e) and (14f) is

$$\begin{aligned} \mathcal{L}(f_{kg}^{rs}, f_{ke}^{rs}, u_g^{rs}, u_e^{rs}) &= \omega \underbrace{\sum_{a \in \mathcal{T}_A} \int_0^{x_a} t_a(\theta) d\theta + \sum_{a \in \mathcal{T}_A^c} \gamma_a E_b x_a}_{\mathcal{L}_1} \\ &+ \underbrace{\sum_{rs} u_g^{rs} \left( q_g^{rs} - \sum_{k \in \mathcal{K}_g^{rs}} f_{kg}^{rs} \right)}_{\mathcal{L}_2} + \underbrace{\sum_{rs} u_e^{rs} \left( q_e^{rs} - \sum_{k \in \mathcal{K}_e^{rs}} f_{ke}^{rs} \right)}_{\mathcal{L}_3} \quad (\text{B.1}) \end{aligned}$$

Therefore, the KKT condition is

$$f_{kg}^{rs} \geq 0, \forall k \in \mathcal{K}_g^{rs}, \forall rs \quad (\text{B.2a})$$

$$f_{kg}^{rs} \frac{\partial \mathcal{L}}{\partial f_{kg}^{rs}} = 0, \forall k \in \mathcal{K}_g^{rs}, \forall rs \quad (\text{B.2b})$$

$$\frac{\partial \mathcal{L}}{\partial f_{kg}^{rs}} \geq 0, \forall k \in \mathcal{K}_g^{rs}, \forall rs \quad (\text{B.2c})$$

$$\sum_{k \in \mathcal{K}_g^{rs}} f_{kg}^{rs} = q_g^{rs}, \forall rs \quad (\text{B.2d})$$

$$f_{ke}^{rs} \geq 0, \forall k \in \mathcal{K}_e^{rs}, \forall rs \quad (\text{B.2e})$$

$$f_{ke}^{rs} \frac{\partial \mathcal{L}}{\partial f_{ke}^{rs}} = 0, \forall k \in \mathcal{K}_e^{rs}, \forall rs \quad (\text{B.2f})$$

$$\frac{\partial \mathcal{L}}{\partial f_{ke}^{rs}} \geq 0, \forall k \in \mathcal{K}_e^{rs}, \forall rs \quad (\text{B.2g})$$

$$\sum_{k \in \mathcal{K}_e^{rs}} f_{ke}^{rs} = q_e^{rs}, \forall rs \quad (\text{B.2h})$$

The value of  $\frac{\partial \mathcal{L}}{\partial f_{kg}^{rs}}$  can be calculated as follows:

$$\begin{aligned} \frac{\partial \mathcal{L}_1}{\partial f_{kg}^{rs}} &= \frac{\partial \left( \omega \sum_{a \in \mathcal{T}_A} \int_0^{x_a} t_a(\theta) d\theta \right)}{\partial x_a} \frac{\partial x_a}{\partial f_{kg}^{rs}} \\ &= \sum_{a \in \mathcal{T}_A} \omega t_a(x_a) \delta_{akg}^{rs} = c_{kg}^{rs} \quad (\text{B.3}) \end{aligned}$$

Moreover,

$$\frac{\partial \mathcal{L}_2}{\partial f_{kg}^{rs}} = \frac{\partial \sum_{rs} u_g^{rs} \left( q_g^{rs} - \sum_{k \in \mathcal{K}_g^{rs}} f_{kg}^{rs} \right)}{\partial f_{kg}^{rs}} = -u_g^{rs} \quad (\text{B.4})$$

Thus, the KKT conditions (B.2a)-(B.2d) are equivalent to

$$f_{kg}^{rs} \geq 0, \forall k \in \mathcal{K}_g^{rs}, \forall rs \quad (\text{B.5a})$$

$$f_{kg}^{rs} (c_{kg}^{rs} - u_g^{rs}) = 0, \forall k \in \mathcal{K}_g^{rs}, \forall rs \quad (\text{B.5b})$$

$$c_{kg}^{rs} - u_g^{rs} \geq 0, \forall k \in \mathcal{K}_g^{rs}, \forall rs \quad (\text{B.5c})$$

$$\sum_{k \in \mathcal{K}_g^{rs}} f_{kg}^{rs} = q_g^{rs}, \forall rs \quad (\text{B.5d})$$

Similarly, the value of  $\frac{\partial \mathcal{L}}{\partial f_{ke}^{rs}}$  can be calculated as follows:

$$\begin{aligned} \frac{\partial \mathcal{L}_1}{\partial f_{ke}^{rs}} &= \frac{\partial \left( \omega \sum_{a \in \mathcal{T}_A} \int_0^{x_a} t_a(\theta) d\theta + \sum_{a \in \mathcal{T}_A^c} \gamma_a x_a E_b \right)}{\partial x_a} \frac{\partial x_a}{\partial f_{ke}^{rs}} \\ &= \sum_{a \in \mathcal{T}_A} \omega t_a(x_a) \delta_{ake}^{rs} + \sum_{a \in \mathcal{T}_A^c} \gamma_a E_b \delta_{ake}^{rs} = c_{ke}^{rs} \quad (\text{B.6}) \end{aligned}$$

The second equation is due to (5), and the last equation is according to the definition of  $c_{ke}^{rs}$ . Moreover,

$$\frac{\partial \mathcal{L}_3}{\partial f_{ke}^{rs}} = \frac{\partial \sum_{rs} u_e^{rs} \left( q_e^{rs} - \sum_{k \in \mathcal{K}_e^{rs}} f_{ke}^{rs} \right)}{\partial f_{ke}^{rs}} = -u_e^{rs} \quad (\text{B.7})$$

Thus, the KKT conditions (B.2e)-(B.2h) are equivalent to

$$f_{ke}^{rs} \geq 0, \forall k \in \mathcal{K}_e^{rs}, \forall rs \quad (\text{B.8a})$$

$$f_{ke}^{rs} (c_{ke}^{rs} - u_e^{rs}) = 0, \forall k \in \mathcal{K}_e^{rs}, \forall rs \quad (\text{B.8b})$$

$$c_{ke}^{rs} - u_e^{rs} \geq 0, \forall k \in \mathcal{K}_e^{rs}, \forall rs \quad (\text{B.8c})$$

$$\sum_{k \in \mathcal{K}_e^{rs}} f_{ke}^{rs} = q_e^{rs}, \forall rs. \quad (\text{B.8d})$$

The (B.5) and (B.8) are exactly the condition for Wardrop User Equilibrium. Furthermore, since  $dt_a(x_a)/dx_a > 0$  and  $dt_a(x_a)/dx_b = 0$ , then  $\frac{\partial^2 \mathcal{L}_1}{\partial x_a^2} = \frac{\omega_a dt_a(x_a)}{\partial x_a} > 0$ ,  $\frac{\partial^2 \mathcal{L}_1}{\partial x_a \partial x_b} = \frac{\omega_a dt_a(x_a)}{\partial x_b} = 0$ . So the Hessian Matrix of  $\mathcal{L}_1$  is a diagonal matrix with the diagonal elements all greater than 0, and is positive definite. The objective function of (14) is strictly convex and its feasible region (14b)-(14f) is also convex. Consequently, problem (14) has a unique optimal solution, and  $x_a, \forall a \in \mathcal{T}_a$  is unique.